Neutron imaging with a Micromegas detector

S Andriamonje [A], V. Dangendorf [B], I. Espagnon [C], H. Friedrich [B], A. Giganon [A], I. Giomataris [A], F. Jeanneau [C*], R. Junca [C], A. Menelle [D], J. Pancin [A], A. Pluquet [C], L. R. Rodríguez [E], M. Voytchev [C]

[A] *DSM/DAPNIA, CEA-Saclay, 91191 Gif sur Yvette Cedex, France*
[B] *PTB, Braunschweig, Germany*
[C] *DRT/DeTeCS, CEA-Saclay, 91191 Gif sur Yvette Cedex, France*
[D] *DSM/DRECAM/LLB, CEA-Saclay, 91191 Gif sur Yvette Cedex, France*
[E] *Dpto de Física, Universidad de Burgos, Avda. Cantabria s/n., 09006 Burgos, Spain*

***Abstract*—Due to its performances for neutron detection, the micropattern gaseous detector Micromegas is designed for neutron imaging. In this paper will be presented new results obtained with thermal neutrons near Orphée reactor at CEA Saclay. The goal of studies with a bi-dimensional detector was to tune different parameters in order to achieve the best spatial resolution which is around 160 µm (defined as the standard deviation) in double amplification mode and 180 µm in classical mode. Several 2D imaging tests have been carried out and an example, which shows different problems inherent in the substrate manufacturing, will be presented.**

Then, a tomographic section of a multi-wires cable, achieved with a one-dimensional Micromegas, will be presented. The high number of pillars sustaining the micromesh has lead to local inefficiencies, disturbing the tomographic reconstruction, but this result, the first tomography carried out with this kind of detector, is very encouraging.

I. Introduction

MICROMEGAS (MICRO-MEsh GAseous Structure) is a gaseous detector developed in Saclay since 1996 [1] and initially designed for fundamental research purposes, specially for detection and localization of charged particles. Several studies have already been performed with this detector [2-5], demonstrating its capacity to work at high particles flux with a good spatial resolution. In this study, the performances of this detector are evaluated for applications in thermal neutron imaging. New results obtained near Orphée facility in Saclay, with a 2D prototype, will be presented. Previous investigations gave promising results in terms of spatial resolution which will introduce a study about 2D imaging and the problems met with the 2D readout plane. A second part will be dedicated to a tomographic section obtained with a Micromegas 1D prototype which have previously achieve a spatial resolution around 60 µm [5].

II. The Micromegas detector

A. Detector principle

When charged particles travel through the gas, electrons are produced between the drift electrode and the micromesh by ionization process. Then they drift towards the micromesh under the action of the electric field (~1 kV/cm) applied in the conversion gap (0.7 mm). After the micromesh, they are multiplied in the narrow amplification gap (50 or 100 µm) – see figure 1 – and the subsequent electron avalanche induces a current on the anode strips.

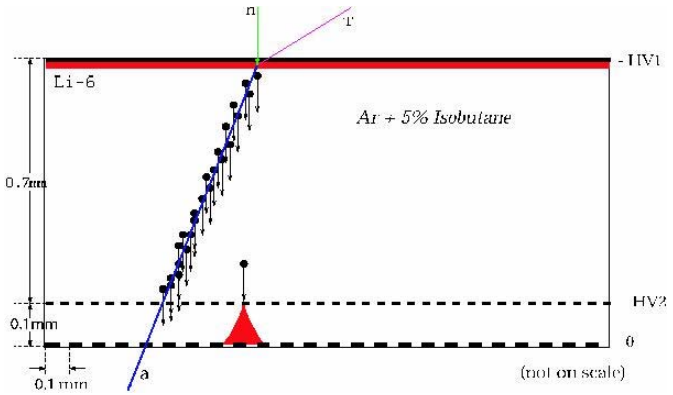

Fig. 1. Micromegas principle for neutron detection.

However, a neutron/charged particle converter is necessary to produce ionization. The conversion reactions used are neutron capture on ^{6}Li (or ^{6}LiF) and ^{10}B (respectively with cross section of 940 and 3840 barns), deposited on the drift electrode:

$$^{6}_{3}Li + n \rightarrow {}^{4}_{2}He(2.05MeV) + {}^{3}_{1}H(2.73MeV) \qquad Q = 4.78 \text{ MeV}$$

$$^{10}_{5}B + n \rightarrow {}^{4}_{2}He(1.47MeV) + {}^{7}_{3}Li(0.83MeV) \qquad Q = 2.7 \text{ MeV}$$

Since the incoming neutron energy is negligible compared to the reaction Q value, the two reactions products (alpha, triton or ^{7}Li) are emitted in opposite directions. The optimal

* Corresponding author: F. Jeanneau; tel: +33-(0)1-69089348; fax: +33-(0)1-69089348; email address: fabien.jeanneau@cea.fr
Manuscript received October 6, 2004.
This work was supported in part by the Conseil Régional d'Ile de France.

thickness of the converter (table 1) has been estimated by simulation in each cases taking into account the exit of the products from the converter (see figure 2 for the ^{6}Li converter).

TABLE I
DIFFERENT CONVERTERS PARAMETERS

Type	^{6}Li (1)	^{6}LiF (2)	^{10}B (3)
Thickness [µm]	100	2 / 24	0.8
Efficiency (%)	18	1.1 / 5.9	3.6
Thickness optimal [µm]	130	33	3.4
Efficiency max (%)	18	6.4	7.8

Evaporated in:
(1) Physikalisch Technische Bundesanstalt (PTB), Braunschweig, Germany
(2) University of Burgos, Spain
(3) CERN, Geneva, Switzerland

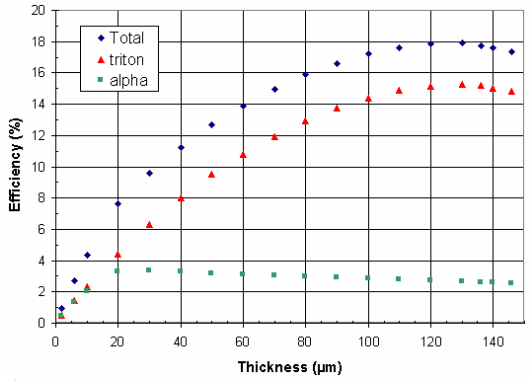

Fig. 2. ^{6}Li conversion efficiency

Conversion products are emitted isotropically so, in order to minimize the strip multiplicity for large angles, the conversion gap is reduced to few hundreds of micrometers; amplification gap is 50 µm high.

Two working modes can be used: normal mode, when amplification takes place in the lower gap, or pre-amplification mode, when the electric field applied in the conversion gap is high enough to amplify the signal so that the global detector gain is a contribution from the two stages.

B. *Electronics and data acquisition system*

For each event, the spatial distribution of the deposited charge on the 384 strips is collected by 4 GASSIPLEX [6] boards (96 channels per board) performing charge preamplification and multiplexing. A VME electronics, composed of a sequencer (*CAEN* model V551) and 2 CRAMs (*CAEN* model V550 - 10 bits), is used to command the GASSIPLEX and store their signals, and the acquisition system is triggered by the amplified micromesh signal. Once all the ADC values have been stored in the CRAMs, data are transferred on a PC via VME-MXI-2 card (National Instruments). The whole system is managed by a *LabView* software allowing a pedestal suppression, in order to acquire data with a higher frequency (around 2.5 kHz).

III. 2D IMAGING STUDY

Tests and measurements have been carried out near Orphée reactor in Saclay. The detector has been irradiated in a 0.025 eV neutron beam of 10^{6} n.cm^{-2}.s^{-1}, after two collimators (B_4C and Cd) defining a 10×10 mm² working area.

A. *Prototype description*

The 2D readout, which is the main part of this 2D prototype, is made on a coppered Kapton where are etched the strips with a pitch of 300 µm. Strips consist in hexagonal pixels connected like on the figure 3, on the upper face in one dimension and on the other face by metallic holes in the second dimension.

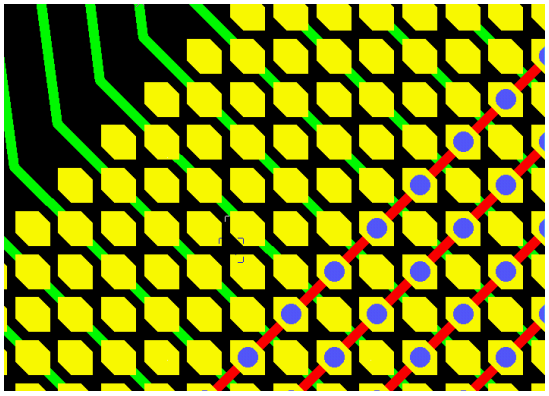
Fig. 3. Plan of the 2D readout (pitch=300µm)

B. *Data analysis*

Once the normal distribution of the electronic noise is registered for each channel (obtained without neutron beam), the mean value of the distribution gives the pedestal value, and the standard deviation will be used to discriminate the signal from the noise. These values are registered in the acquisition system so that it will record the channels with an ADC value larger than the pedestal value plus typically 3 rms. Empty channels are then suppressed before registration, minimizing the data flow and allowing the acquisition system to run at higher frequency.

The data file contains the event number and the list of the fired strips with their ADC value. Every contiguous strips with a signal is stored in a cluster by a C++ code which corrects eventually dead strips by the mean value of their neighbours. The main cluster is the one which contains the higher charge strip and several parameters are needed from this cluster: charge and number of the maximum strip, total number of strips, total charge (sum of all ADC values) and the barycentre of the cluster charge, which is related to the incident neutron position. Using these parameters it is possible to reconstruct the incident neutron beam on the plane of strips, and to improve the spatial resolution and so the image quality, by applying cuts on the cluster charge or multiplicity.

The selection criteria are:

- at least one cluster in X AND Y

- cluster multiplicity: in order to limit the error on the barycentre calculation, only low multiplicity (2, 3 or 4 strips) are considered
- charge: no saturation strips

C. *Spatial resolution estimation*

In order to determine the spatial resolution of the detector, an image with neutrons of a calibrated object is used, here a hole (∅ 0.6 mm) in a Cadmium foil (thickness 0.8 mm). The image is fitted by the convolution of a square function and a Gaussian function:

$$T(x,y) = p + A\left(Erf\left(\frac{a+\sqrt{(x-\mu_x)^2+(y-\mu_y)^2}}{\sqrt{2}\sigma}\right) + Erf\left(\frac{a-\sqrt{(x-\mu_x)^2+(y-\mu_y)^2}}{\sqrt{2}\sigma}\right)\right)$$

where p is the noise level, A is a constant, a is the half width of the hole, μ_x and μ_y are the centers of the hole and σ is the gaussian r.m.s. and gives the spatial resolution value.

D. *Results*

Figure 4 and 5 show the image and profile of 0.6 mm holes. The plane of strips was containing a lot of dead strips and the spatial resolution study was carried out using a small working zone (10×10 mm² centered on the images of the holes).

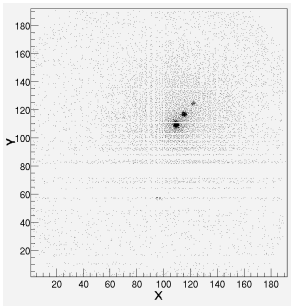

Fig. 4. Images of 0.6 mm holes obtained on the whole surface of the detector

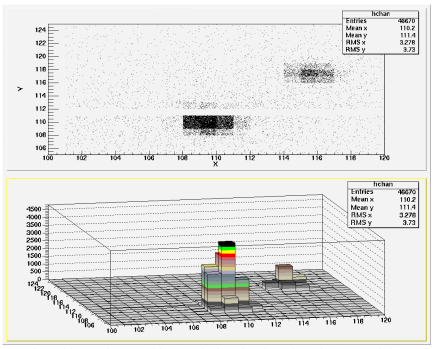

Fig. 5. Closer detail and profiles of the holes in the working zone

Following results have been calculated with the hole presenting less statistics because of the dead strip passing through the other one (see figure 5). Figure 6 shows the 1D (Y) resolution variations as a function of event selection (cluster multiplicity).

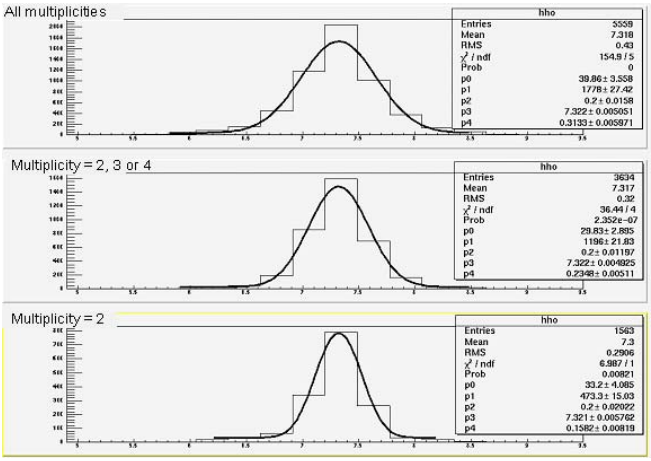

Fig. 6. 1D spatial resolution for different cluster multiplicities.

The optimal resolution is around 160 µm and is obtained for a multiplicity equals to 2, as it is represented on the figure 7.

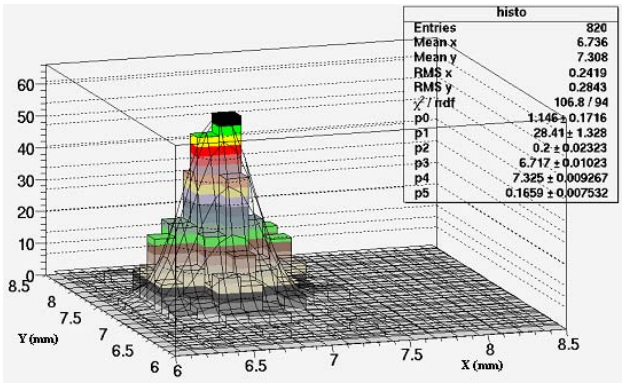

Fig. 7. 2D spatial resolution for multiplicity of 2

Events selection is quite hard to obtain an optimal spatial resolution, so the number of events conserved after selection, and the global efficiency of the detector, is decreasing from a resolution around 300 µm, with 90 % of good events, to a resolution around 160 µm, with only 15 % of events kept.

Two different working modes have been studied as it is said before. Better results, in terms of spatial resolution, are obtained in pre-amplification mode, and that can be explained by a better neutron position reconstruction due to the shape of the clusters (see figure 8). In normal mode, electrons created along the way of the particle in the conversion gap will lead to a uniform signal. On the other hand, in pre-amplification mode, electrons created at the beginning of the conversion gap, and corresponding exactly to the neutron position, have a bigger contribution to the signal. The cluster barycentre is then shifted towards the particle entry point, and then will affect the spatial resolution.

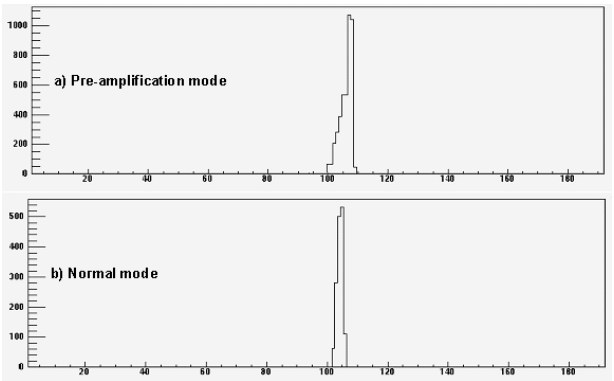

Fig. 8. Shape of the charge cluster in pre-amplification and normal mode

Finally, the 2D spatial resolution is about 180 µm in normal mode and 160 µm in pre-amplification mode with an acceptation rate of 15 %.

A new prototype has been mounted with a new plane of strips in order to perform an image of a real object: a Gadolinium foil of 100 µm thick on which have been etched the letters "CEA". Figure 9 shows the scheme of the etching and the image obtained in neutron beam.

The three letters of the object are well reconstructed, and the dimensions respected, but the image quality is not very good because of inefficiency area. After a carefully electric test of the plane of strips, some cross-talk between the strips of the 2 directions has been found out, causing significant signal losses on some strips. Cluster barycentre is then affected by this effect which degrades spatial resolution and response homogeneity. Nevertheless these results are very encouraging and a special attention is carried on the manufacturing of the new plane of strips in order to improve the 2D performances of this detector.

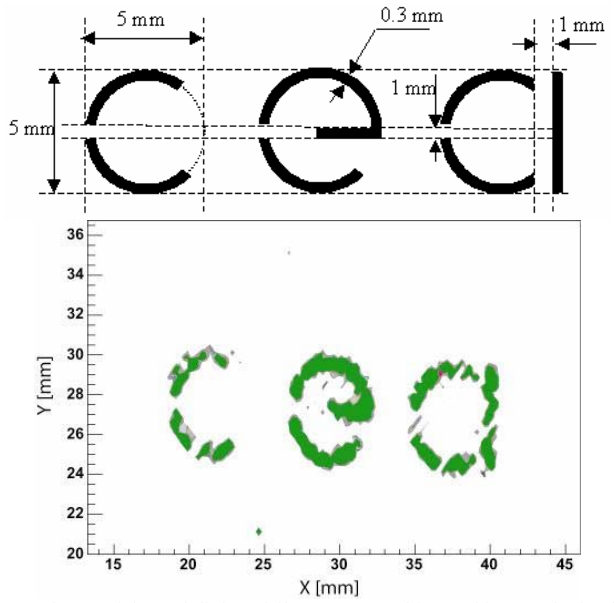

Fig. 9. Scheme of the gadolinium foil (100 µm) etching and image obtained with the detector.

IV. Tomography with a 1D Micromegas detector

A. Setup description

Measurements for tomography have been performed in march 2004 at GKSS in Geesthacht, Germany, near the GeNF (Geesthacht Neutron Facility) reactor which is dedicated to neutron spectroscopy with 15 experimental areas, like POLDI area (POLarised DIffractometer) delivering a thermal neutron flux of 8.10^4 n.cm^{-2}.s^{-1} with an optimal L/D ratio around 2000. The tomographic section of a multi-wires cable (∅ 6 mm), containing 12 wires (∅ 0.5 mm each), has been achieved using a 1D Micromegas (same principle than before but with a 1D readout plane of strips). Between the object and the detector is located a 1 mm wide slit in order to reduce scattered neutrons (see figure 10).

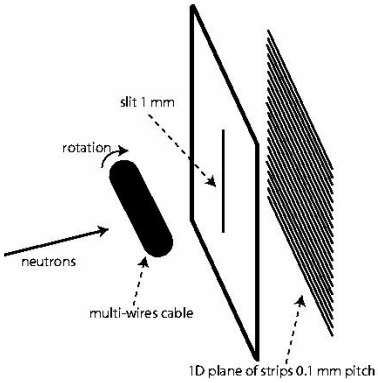

Fig. 10. Schematic view of the tomographic setup (not on scale)

A remote control motor hold and rotate the object between each projections.

B. Tomography test results

The total number of projections is 81, on 360°, with a counting rate around 200 neutrons per seconds and per projection. The time allocated for each projections is about 1000 secondes and so a tomographic section can be performed in about 26 hours.

Because of a poor statistics, it was not possible to apply the event selection necessary to reach the optimal resolution (keeping only the low multiplicity events). Cuts in our case are: a multiplicity below 12 strips and no events with a too high deposited charge per strip, in order to select the event perpendicular to the direction of the strips. These cuts ensure a spatial resolution around 100 µm, calculated with the image of a slit of 500 µm wide parallel to the strips.

An image of the beam with no object $I_0(x)$ is needed for the tomographic reconstruction to monitor the beam and the defects of the detector. Each projection $I^i(x)$ is normalized with the empty run, by adjusting the number of events on the edges of the object, so that the beam or acquisition time variations are corrected. Then the ratio $Log(I_0(x)/I^i(x))$ gives an evaluation of the integral of the neutron attenuation coefficient in the projection direction, as it is represented on figure 11 for the projection at 0°. Some structures due to the wires in the cable are visible but the normalization is not enough efficient

to remove totally the influence of the pillars sustaining the micromesh.

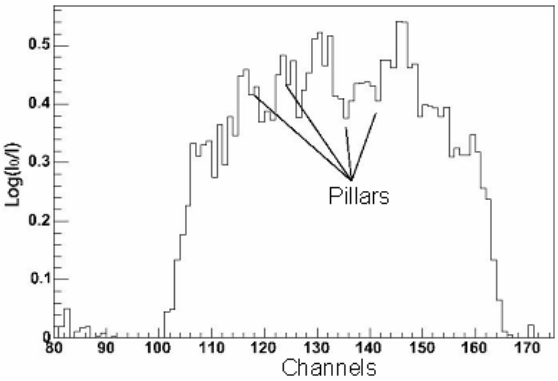

Fig. 11. Projection at 0° after normalization.

The reconstruction is represented on the figure 12 (bottom) with the sinogram corresponding to the piling of the projections on the left. Some wires and the sheath are well reconstructed but the image center is quite blurred. As a comparison, the section of the same object obtained with image plates is better (see figure 12 – right).

The main reason to explain this difference of quality is certainly the high number of pillars on the plane of strips, deposited every 0.6 mm, which could be decreased by a factor 4. Local inefficiencies due to pillars are interpreted as concentric circles, degrading the spatial resolution, specially near the rotation center.

Another reason is the lack of statistics and the fact that the optimal set of cuts cannot be applied to achieve the best spatial resolution, but this could be improved using a higher neutron flux.

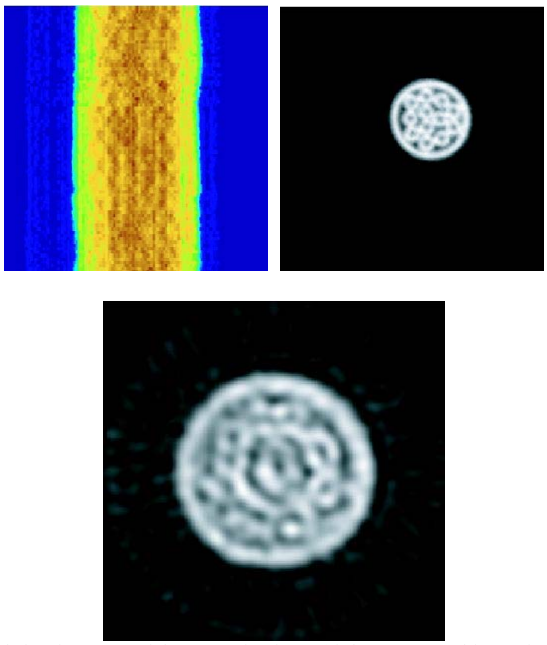

Fig. 12. (left) Sinogram of the 81 projections, (right) tomographic section using image plates, (bottom) tomographic section using the Micromegas detector.

V. Conclusion

The 2D prototype equipped with its acquisition electronics worked well during the experiments near Orphée reactor. A 2D spatial resolution of around 160 µm (in terms of standard deviation) has been reached in pre-amplification mode and around 180 µm in normal mode, with an acceptation level of 15 % (multiplicity equals to 2 in X and in Y). Taking into account the dead strips, these results are very encouraging.

An image has been performed with a new plane of strips and has permitted to detect cross-talk between the 2 directions of the plane of strips. Manufacturing process is optimized to avoid this kind of defects which degrades the spatial resolution and leads to local inefficiencies, some strips loosing the main part of their signal. Further measurements are necessary.

A tomographic section has been carried out with a 1D prototype near the GKSS reactor in Geesthacht. The image of a multi-wires cable obtained after reconstruction do not present the same quality than the one obtained with image plate. The main reason is the high number of pillars on the plane of strips, leading to local inefficiencies and then to artefacts in the reconstruction process. Moreover, it was not possible to apply the optimal set of cuts due to the lack of statistics. The results obtained are very encouraging despite the technical problems encountered. Decreasing the number of pillars and using a more high neutron flux could be simple solutions to perform new measurements and conclude about the relevance of this kind of devices for neutron imaging.

VI. References

[1] I. Giomataris, Ph. Rebourgeard, J.-P. Robert, and G. Charpak, "Micromegas: a high-granularity position-sensitive gaseous detector for high particle-flux environments," *Nuclear Instruments and Methods in Physics Research A 376* (1996) 29-35.

[2] J. Pancin et al., "Measurement of the n-TOF beam profile with a Micromegas detector," *Nuclear Instruments and Methods in Physics Research A 524* (2004) 102-114.

[3] J. Derré, I. Giomataris, Ph. Rebourgeard, H. Zaccone, J.-P. Perroud, and G. Charpak, "Fast signals and single electron detection with a Micromegas photodetector," *Nuclear Instruments and Methods in Physics Research A 449* (2000) 314-322.

[4] J. Derré, I. Giomataris, "Recent experimental results with Micromegas," *Nuclear Instruments and Methods in Physics Research A 477* (2002) 23-28.

[5] S. Andriamonje et al., "Comparison between image plate and Micromegas detector for thermal neutron tomography," *Advances in Neutron Scattering Instrumentation,* Proceedings of SPIE, Volume 4785 (2002).

[6] J.-C. Santiard et al., CERN-ECP/94-17.